

# Optical Engineering

OpticalEngineering.SPIEDigitalLibrary.org

## **Measurement and comparison of one- and two-dimensional modulation transfer function of optical imaging systems based on the random target method**

Jiqiang Kang  
Qun Hao  
Xuemin Cheng

# Measurement and comparison of one- and two-dimensional modulation transfer function of optical imaging systems based on the random target method

Jiqiang Kang,<sup>a</sup> Qun Hao,<sup>b</sup> and Xuemin Cheng<sup>a,\*</sup>

<sup>a</sup>Tsinghua University, Graduate School at Shenzhen, Department of Precision Instrument, Shenzhen 518055, China

<sup>b</sup>Beijing Institute of Technology, School of Optoelectronics, Beijing 100081, China

**Abstract.** One-dimensional modulation transfer function (1-D MTF) has been generally calculated to evaluate the image quality of optical imaging systems, such as the horizontal MTF and vertical MTF. These MTFs can be measured by the use of some mature ways. However, the information of 1-D MTF for performance evaluation may not be enough for the systems handling two-dimensional (2-D) targets of high resolution, thus discussing 2-D MTF will be necessary. We investigate the measurement method for the 1-D and 2-D MTF of optical imaging systems based on the random target method, and the characteristics of 2-D MTF and 1-D MTF in terms of MTF values and cutoff frequency are also noted. © The Authors. Published by SPIE under a Creative Commons Attribution 3.0 Unported License. Distribution or reproduction of this work in whole or in part requires full attribution of the original publication, including its DOI. [DOI: [10.1117/1.OE.53.10.104105](https://doi.org/10.1117/1.OE.53.10.104105)]

Keywords: image quality evaluation; modulation transfer function; random image; liquid-crystal display; fast Fourier transform; power spectral density.

Paper 140973 received Jun. 18, 2014; revised manuscript received Sep. 16, 2014; accepted for publication Sep. 26, 2014; published online Oct. 30, 2014.

## 1 Introduction

Modulation transfer function (MTF) has been widely used to evaluate the image quality of imaging systems because it works in a direct way to reveal the performance of imaging systems.<sup>1-3</sup> MTF describes the spatial frequency transfer characteristics of imaging systems from object space to image space by employing the contrast value of a series of sine waves with varying spatial frequencies.

There are a lot of mature ways to measure the MTF of optical imaging systems. According to their different templates, MTF test methods can be categorized into different types, such as the knife edge method,<sup>4</sup> the slit method,<sup>5</sup> the bar target method,<sup>6-8</sup> etc. Generally, these methods' templates have a common feature in that their image brightness changes in one direction and remains constant in the orthogonal direction, e.g., the U.S. Air Force resolution target. Naturally, the MTF measured with these templates will contain the modulation information in only one direction, such as the horizontal MTF and vertical MTF. In this paper, these MTFs are called one-dimensional (1-D) MTFs and their corresponding templates are called 1-D templates.

In 2010, Marom et al.<sup>9</sup> proposed a new kind of two-dimensional (2-D) template which looks like a checkerboard measuring the "true characterization" of some systems, for example, the barcode scanning system. Marom et al. explained that a 2-D template is different from a 1-D template because its image brightness changes in two orthogonal directions, and the result of a 1-D contrast transfer function (CTF) for a 2-D template will be affected by the brightness changes in another direction, which will not occur with the 1-D template. Haim et al. proved theoretically and experimentally

that the CTF measured by the 2-D template is lower than that obtained with 1-D templates at every spatial frequency and at its cutoff frequency while the former template is  $1/\sqrt{2}$  times the latter one.<sup>10,11</sup> To maintain consistency, in this paper we adopt Marom's 2-D template definition in which the brightness of 2-D templates changes in two orthogonal directions. The MTF that simultaneously contains the modulation information in two orthogonal directions is called the 2-D MTF.

Recently, the random target method, a new MTF test method, has been applied for image quality evaluation. The method was first proposed by Daniels et al.<sup>12</sup> in which a random image is used as the template, and then it is imaged on a charge coupled device (CCD) by the optical system under test (OSUT). By using the power spectral density (PSD) values of the image captured by a CCD and those of the original image, one can obtain the optical system's MTF with Fourier spectral analysis. The test method is convenient and fast,<sup>13</sup> because the random image has the characteristic of shift invariance,<sup>14</sup> and one can easily achieve automatic measurement. The previous works focus mostly on the 1-D MTF test.<sup>9-13,15-18</sup> However, the random image can also be used as a 2-D target since its image brightness changes in two orthogonal directions and is available for measuring 2-D MTF. In 2013, Evtikhiev et al.<sup>19</sup> proposed a new random target to reduce the noise impact for the 2-D MTF measurement.

In this paper, we investigate the measurement for 2-D MTF with the random target method as well as 1-D MTF. A new approach is applied to reduce noise by the use of a significantly large number of random images. The results of the measurement for 1-D and 2-D MTF show that 2-D MTF can be more comprehensive than 1-D MTF when describing the true modulation features of optical imaging systems.

Section 2 analyzes the 1-D and 2-D MTF theoretically and elaborates on the mathematical principles for 1-D and 2-D MTF measurement by using the random target method.

\*Address all correspondence to: Xuemin Cheng, E-mail: [chengxm@sz.tsinghua.edu.cn](mailto:chengxm@sz.tsinghua.edu.cn)

Section 3 presents the procedures of the experiment and the results. Section 4 contains the conclusions.

## 2 Methodology

### 2.1 MTF Review and Comparison of 1-D and 2-D MTF

In incoherent illumination systems, the optical transfer function (OTF) is the normalized autocorrelation of the system exit pupil, which can be expressed as

$$\text{OTF}(\xi, \eta) = \frac{\iint_{-\infty}^{\infty} P(x, y)P^*(x + \lambda z_i \xi, y + \lambda z_i \eta) dx dy}{\iint_{-\infty}^{\infty} P(x, y) dx dy}, \quad (1)$$

where  $P(x, y)$  is the system's exit pupil function,  $\lambda$  is wavelength, and  $z_i$  is the distance from the exit pupil plane to the image plane. MTF is the absolute value of the system's OTF, i.e.,  $\text{MTF} = |\text{OTF}|$ . This is the rigorous definition of MTF. Although one rarely measures MTF through OTF because the OTF test itself is complicated, there is no denying that it is plausible.

MTF describes the spatial frequency transfer characteristics of imaging systems defined as the ratio of the output to the input sinusoidal targets' contrast value. In this way, one can easily obtain the MTF through detecting the contrast value of input and output sinusoidal targets, but this method is rarely used because it is hard to exactly and efficiently fabricate sinusoidal targets. In our work, to reveal the internal relationship of the 1-D and 2-D MTF of the optical system, the sinusoidal targets are applied by use of Fourier transform.

At first, we analyze the 1-D MTF with a typical 1-D sinusoidal template which is shown in Fig. 1(a) and its expression is

$$I_{\text{input}}^{1\text{-D}} = \frac{1}{2} [1 + \sin(2\pi x f)], \quad (2)$$

where  $f$  is the spatial frequency, and  $f = 1/(2a)$ . If we treat the OSUT as a linear time-invariant system, then the input sinusoidal signal will be modulated by the system's MTF when it transmits through the system, and the output signal will be

$$\begin{aligned} I_{\text{output}}^{1\text{-D}} &= \frac{1}{2} [1 + \sin(2\pi x f) \cdot \text{MTF}_{1\text{-D}}(f)] \\ &= \frac{1}{2} \left[ 1 + \sin\left(\frac{\pi x}{a}\right) \cdot \text{MTF}_{1\text{-D}}\left(\frac{1}{2a}\right) \right], \end{aligned} \quad (3)$$

where  $\text{MTF}_{1\text{-D}}(f)$  is the 1-D MTF value at spatial frequency  $f$ .

The 2-D case is more complex than that of the 1-D. A typical 2-D sinusoidal target is shown in Fig. 1(b), which can be expressed as

$$I_{\text{input}}^{2\text{-D}} = \frac{1}{2} [1 + \sin(2\pi x f_x) \cdot \sin(2\pi y f_y)], \quad (4)$$

where  $f_x$  and  $f_y$  are the fundamental frequencies along the horizontal and vertical directions, and  $f_x = f_y = 1/(2a)$ . As for the 2-D target, we also need to obtain the output signals when input signals transmit through the optical system by analyzing its 2-D spectrum with 2-D Fourier transform, as in Eq. (5). Its spectrum is shown in Fig. 2.

$$\begin{aligned} H(\xi, \eta) &= \frac{1}{2} \left\{ 1 + \frac{1}{4} [\delta(\xi - f_x) - \delta(\xi + f_x)] \right. \\ &\quad \left. \cdot [\delta(\eta + f_y) - \delta(\eta - f_y)] \right\} \\ &= \frac{1}{2} \left\{ 1 + \frac{1}{4} [\delta(\xi + f_x, \eta - f_y) + \delta(\xi - f_x, \eta + f_y) \right. \\ &\quad \left. - \delta(\xi + f_x, \eta + f_y) - \delta(\xi - f_x, \eta - f_y)] \right\}. \end{aligned} \quad (5)$$

Equation (5) shows that 2-D target contains different frequency components in the 2-D frequency domain, and indicates the modulation features of the imaging system in the 2-D target case when adopting the 2-D MTF.

In Fig. 2, one can easily note that four different frequency components uniformly distribute on a circle whose radius is  $f = (f_x^2 + f_y^2)^{1/2}$ . In terms of an ideal axis symmetrical system (aberration-free), its 2-D MTF values will be equal to all the frequency points on the circle which can be calculated with equation

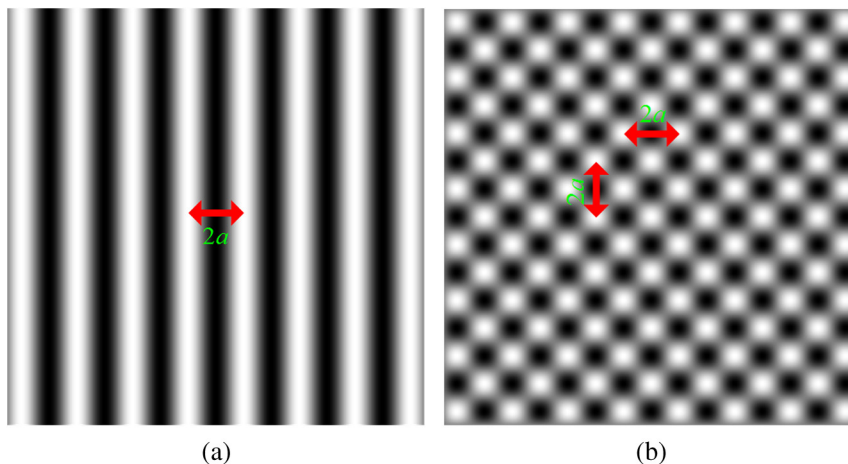


Fig. 1 Typical sinusoidal targets: (a) one-dimensional (1-D) target, (b) two-dimensional (2-D) target.

$$\text{MTF}_{2\text{-D}}(f_x, f_y) = \text{MTF}_{1\text{-D}}\left(\sqrt{f_x^2 + f_y^2}\right), \quad (6)$$

where  $\text{MTF}_{2\text{-D}}(f_x, f_y)$  is the 2-D MTF of the system at frequency  $(f_x, f_y)$ . Based on Eq. (6), the output signal of the system is

$$\begin{aligned} I_{\text{output}}^{2\text{-D}} &= \frac{1}{2} [1 + \sin(2\pi x f_x) \cdot \sin(2\pi y f_y) \cdot \text{MTF}_{2\text{-D}}(f_x, f_y)] \\ &= \frac{1}{2} \left[ 1 + \sin\left(\frac{\pi x}{a}\right) \cdot \sin\left(\frac{\pi y}{a}\right) \cdot \text{MTF}_{1\text{-D}}\left(\frac{\sqrt{2}}{2a}\right) \right]. \end{aligned} \quad (7)$$

If we focus the distribution on the horizontal direction ( $\hat{x}$ ) at the center of a row, say  $y = a/2$ , then Eq. (7) becomes

$$I_{\text{output}}^{2\text{-D}} = \frac{1}{2} \left[ 1 + \sin\left(\frac{\pi x}{a}\right) \cdot \text{MTF}_{1\text{-D}}\left(\frac{\sqrt{2}}{2a}\right) \right]. \quad (8)$$

Equations (7) and (8) give the two directions and the ( $\hat{x}$ ) direction's expressions, respectively, of the 2-D output of the system. By comparing Eq. (3) with Eq. (8), one can note that although both of them have the same input expression, they are modulated differently which leads to different outputs. As the image brightness of a 2-D target changes in two orthogonal directions and a 1-D target changes in only one direction, the brightness change in the ( $\hat{y}$ ) direction of the 2-D output will influence the MTF result; this will not happen to the 1-D target when one analyzes the ( $\hat{x}$ ) direction's MTF with the output images. Actually, this interaction of two orthogonal directions is more in line with the actual situation as most systems are used in a 2-D imaging scene which has abundant spatial frequencies distributed in 2-D frequency domain. Therefore, to evaluate the true resolving power of imaging systems, one should apply 2-D targets and adopt 2-D MTF as they can provide comprehensive modulation information about the imaging system.

Moreover, in ideal systems (aberration-free), we build the relationship between the 1-D and the 2-D MTF theoretically, shown in Eq. (9), which is also true in the vertical direction ( $\hat{y}$ ).

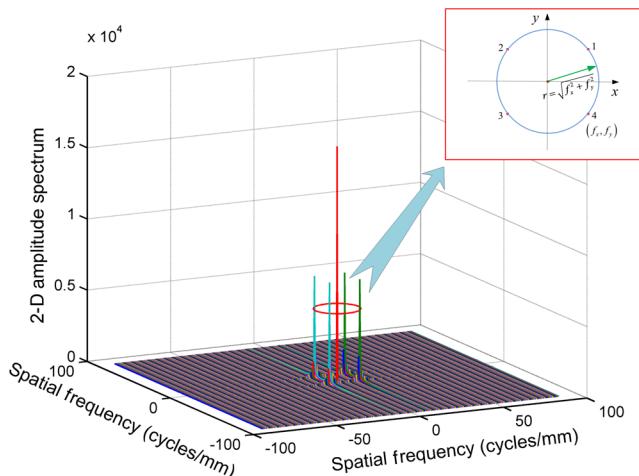


Fig. 2 2-D frequency spectrum of a 2-D sinusoidal target.

$$\text{MTF}_{\hat{x}}^{2\text{-D}}(f) = \text{MTF}_{\hat{x}}^{1\text{-D}}\left(\sqrt{2}f\right). \quad (9)$$

Furthermore, we can deduce from Eq. (9) that the 2-D MTF values are lower than the 1-D MTF values in the corresponding direction and the relationship of their cutoff frequency is

$$f_{\text{CF}}^{2\text{-D}} = f_{\text{CF}}^{1\text{-D}} / \sqrt{2}, \quad (10)$$

where  $f_{\text{CF}}^{2\text{-D}}$  and  $f_{\text{CF}}^{1\text{-D}}$  are the cutoff frequencies of 2-D and 1-D MTF, respectively. This conclusion is made for the case of ideal systems. In the following sections, we will discuss the values of the experimental result.

## 2.2 Random Target Method and Noise Reduction Approach

As stated above, a 2-D target can provide comprehensive information for the 2-D MTF measurement of optical imaging systems in 2-D imaging scenes. However, a selective 2-D target will improve the measurement efficiency of the 2-D frequency. It is appropriate to use random images because, in addition to the advantages stated in Sec. 1, one can easily obtain its 2-D frequency spectrum through 2-D fast Fourier transform (FFT). A pixels random image is shown in Fig. 3 and its 1-D and 2-D PSD are shown in Figs. 4(a) and 4(b).

Random images are generated by a random number generator. Although a random target method is performed, a series of random images are displayed in a liquid crystal display (LCD) one by one which are imaged by the OSUT on a CCD. By calculating the ratio of the output image captured by the CCD to the input random image's PSD, one can get the system's MTF. The mathematical principle of this process could be described as

$$\text{PSD}_{\text{output}} = [\text{MTF}_{\text{sys}} \times \text{MTF}_{\text{test}}]^2 \times \text{PSD}_{\text{input}}, \quad (11)$$

where output PSD and input PSD are the PSDs of the final images and the original images on the LCD.  $\text{MTF}_{\text{sys}}$  and

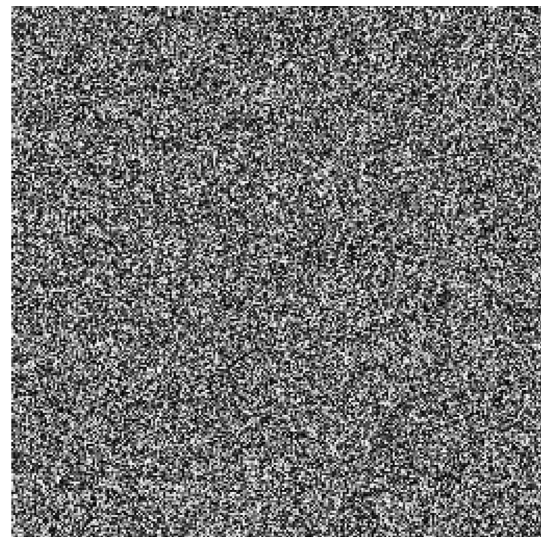
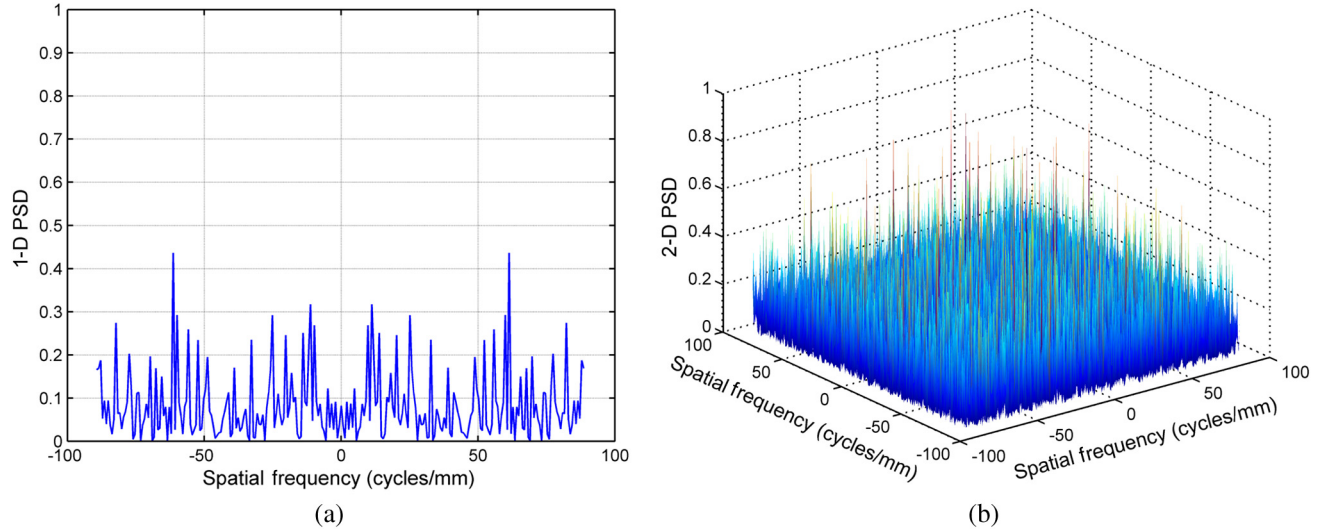


Fig. 3 A 256 × 256 pixel random image.



**Fig. 4** PSD of a random image: (a) 1-D PSD and (b) 2-D PSD.

$MTF_{\text{test}}$  are the system inherent MTF of the system devices (including LCD and CCD) and the OSUT.

Here, to reduce the influence of temporal and spatial noises of the experimental setup,  $PSD_{\text{output}}$  is determined by

$$PSD_{\text{output}} = PSD_{\text{captured}} - PSD_{\text{system}}, \quad (12)$$

where  $PSD_{\text{captured}}$  is the PSD value measured with random images in the screen, while  $PSD_{\text{system}}$  is the PSD value measured without random images in the screen.

In 1-D and 2-D MTF measurements, we should calculate the PSDs of the input and output images, respectively. Then, Eq. (11) becomes

$$PSD_{\text{output}}^{1-D}(f) = [MTF_{\text{sys}}^{1-D}(f) \cdot MTF_{\text{test}}^{1-D}(f)]^2 \cdot PSD_{\text{input}}^{1-D}(f). \quad (13)$$

$$PSD_{\text{output}}^{2-D}(\xi, \eta) = [MTF_{\text{sys}}^{2-D}(\xi, \eta) \cdot MTF_{\text{test}}^{2-D}(\xi, \eta)]^2 \cdot PSD_{\text{input}}^{2-D}(\xi, \eta). \quad (14)$$

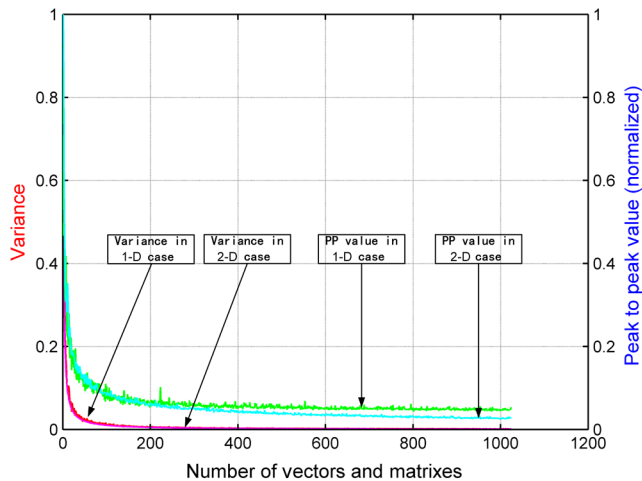


**Fig. 5** Relationship between pp value (normalized at 1 vector or matrix) and variance with the number of vectors and matrices.

1-D and 2-D PSD can be obtained by applying 1-D FFT and 2-D FFT to the images. At the same time, the noise reduction method is applied to obtain a smooth 1-D MTF curve and 2-D MTF surface by taking average of the FFT results for a large number of images. Equations (15) and (16) describe the calculation process in detail

$$PSD_{1-D} = \frac{1}{M_1} \sum_{i=1}^{M_1} \{\text{abs}[\text{FFT}(A_i)]^2 / N_1\}, \quad (15)$$

$$PSD_{2-D} = \frac{1}{M_2} \sum_{j=1}^{M_2} \{\text{abs}[\text{FFT2}(B_j)]^2 / N_2^2\}, \quad (16)$$

where  $A$  is a set of  $1 \times N_1$  vectors, and  $A_i$  means the  $i$ 'th vector.  $B$  is a set of  $N_2 \times N_2$  matrices and  $B_j$  represents the  $j$ 'th matrix of  $B$ .  $M_1$  and  $M_2$  are the numbers of vectors or matrices of  $A$  and  $B$  where  $\text{abs}$  is the function for obtaining an absolute value.

We also discuss the relationship between the variances and peak to peak values of  $PSD_{1-D}$  and  $M_1$ , and the relationship between the variances and peak to peak values of  $PSD_{2-D}$  and the  $M_2$ , as are shown in Fig. 5. The variances are stable when increasing the number of vectors and matrices, which implies that  $M_1 = 1024$  vectors and  $M_2 = 1024$  matrices are sufficient for 1-D and 2-D MTF analysis. The average results of 1-D and 2-D PSD are shown in Figs. 6(a) and 6(b).

### 3 Experiment and Results

#### 3.1 Experimental Setup and Experimental Procedure

The schematic diagram of the experimental setup is shown in Fig. 7. A host with two LCDs is adopted. Monitor 1 is used to show the interactive interfaces of applications and monitor 2 is used to present the random images. Thus the parameters are defined, e.g.,  $l$  and  $d$  are the pixel size of the LCD and CCD, respectively, and  $M$  is the reduction ratio of the optical system.

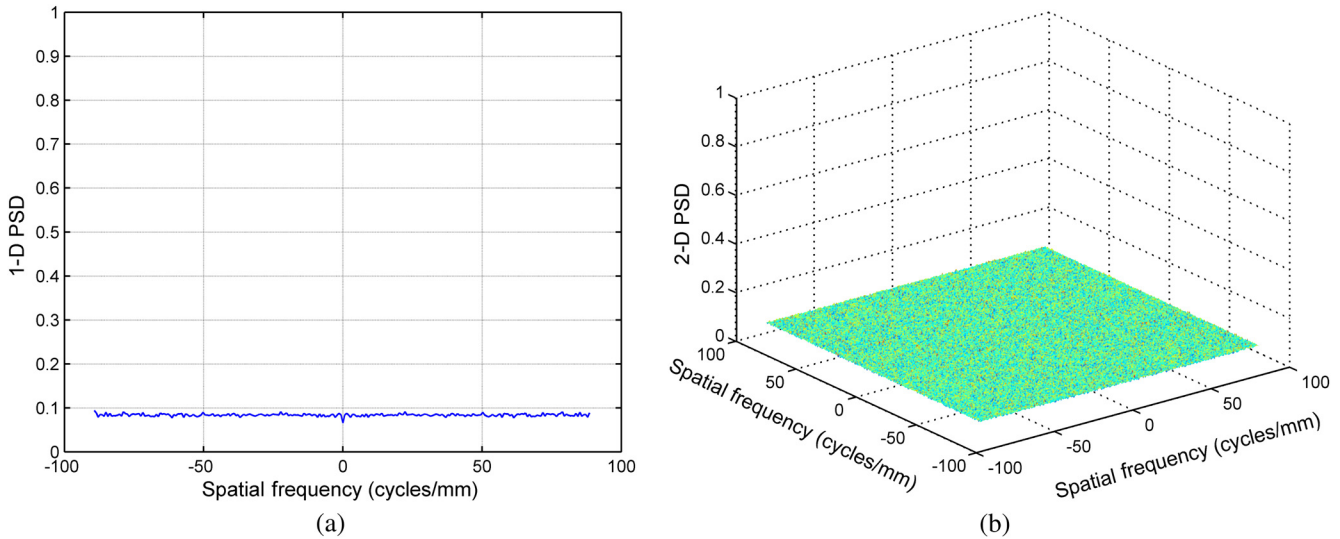


**Fig. 6** Average results: (a) 1-D PSD averaged on 1024 vectors and (b) 2-D PSD averaged on 1024 matrixes.

According to the sampling theorem, to avoid aliasing effects one should ensure  $f_{\max}^s < f_N^c$  since the highest spatial frequency of the LCD measured in the image plane is  $f_{\max}^s = 1/(2 \times l \times M)$  and the Nyquist frequency of the CCD is  $f_N^c = 1/(2 \times d)$ .

In our experiment, monitors 1 and 2 are Samsung SyncMaster E1920W LCDs whose pixel size is 0.2835 mm with a total of  $1440 \times 900$  pixels. The CCD placed in the image plane is a  $1/4$  in. Sony ICX618 monochrome CCD. Its total number of pixels is  $656 \times 492$  with each pixel size being  $5.6 \mu\text{m} \times 5.6 \mu\text{m}$ . Therefore, according to the constraints, the optical system's reduction ratio could not be smaller than 0.0197. In this paper, the reduction ratio of the OSUT is 0.02 and the highest frequency of the screen measured in the image plane is  $1/(2 \times 0.2835 \times 0.02) \approx 88.2$  cycles/mm.

The block diagram of the experiment is shown in Fig. 8. First of all, the CCD captures a series of images without random images displayed in the screen. Also, these captured images will be used to calculate the temporal and spatial noises ( $\text{PSD}_{\text{sys}}$ ) of the experimental setup. Then,  $M_2 = 1024$  random images are displayed on monitor 2 one by one. These  $N \times N$  random images are generated in MATLAB by using the functions named rand and imshow, and we set  $N = 256$  here because it is precise enough for the

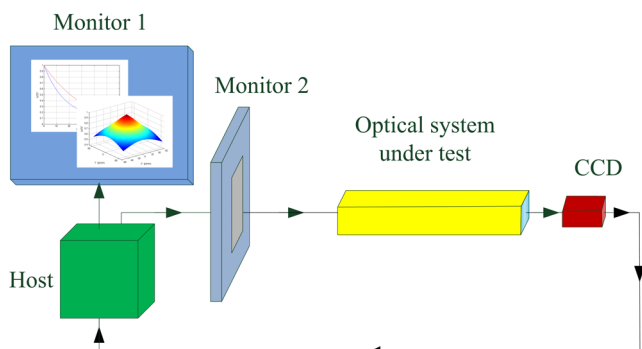


**Fig. 7** Schematic diagram of the experimental setup.

measurement, see Ref. 13. The original random image and the image captured by the CCD are saved in the host. Finally, all the images are used to calculate the 2-D PSD, i.e.,  $\text{PSD}_{\text{measured}}^{2-D}$ , and  $M_1 = (M_2/N)$  images of them are used to calculate the 1-D PSD, i.e.,  $\text{PSD}_{\text{measured}}^{1-D}$ . After acquiring these PSD values, we can calculate the values of the optical system's 1-D and 2-D MTF based on Eqs. (13) and (14).

### 3.2 Results and Discussion

A random image on the screen and its image captured by the CCD are shown in Fig. 9. The 1-D MTF in the horizontal direction is shown in Fig. 10 and the 2-D MTF is shown in Fig. 11. The 1-D MTF and the curve of 2-D MTF in the ( $\hat{x}$ ) direction are plotted in Fig. 12.

In Fig. 12, one can easily note that for a practical system, the 2-D MTF values are lower than the 1-D MTF values at every spatial frequency point. The 1-D MTF's value is 0.023 at the cutoff frequency point. If we set 0.023 as the cutoff value, then the cutoff frequency of the 2-D MTF is 65.9 cycles/mm. Thus  $88.2/65.9 = 1.34$ , which approximates  $\sqrt{2}$ . These results are consistent with the conclusions for an ideal system.

According to Eq. (9), another curve, the ideal curve, is also illustrated in pink in Fig. 12. The value for the ideal

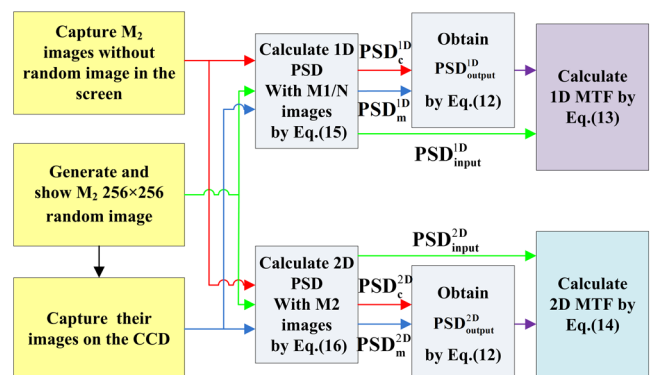


**Fig. 8** Block diagram of experimental procedures.

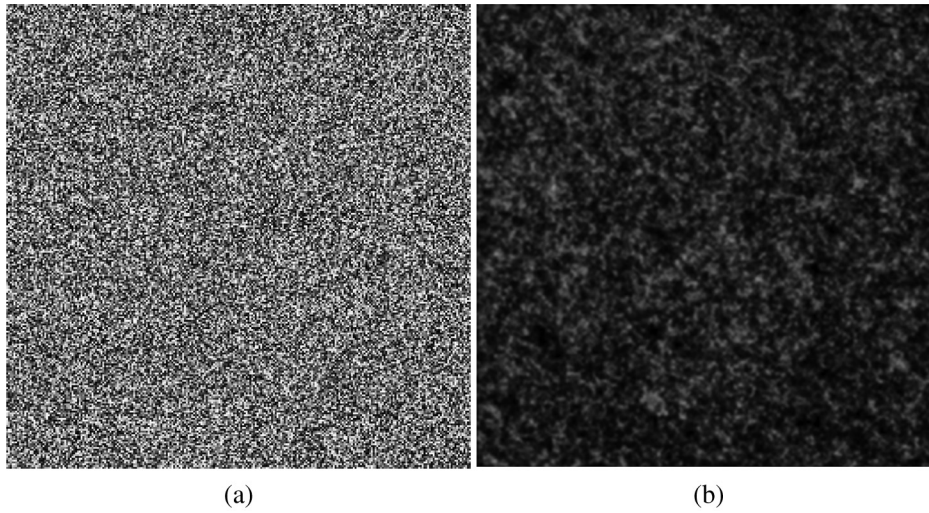


Fig. 9 (a) Random image on the screen. (b) Image captured by the CCD.

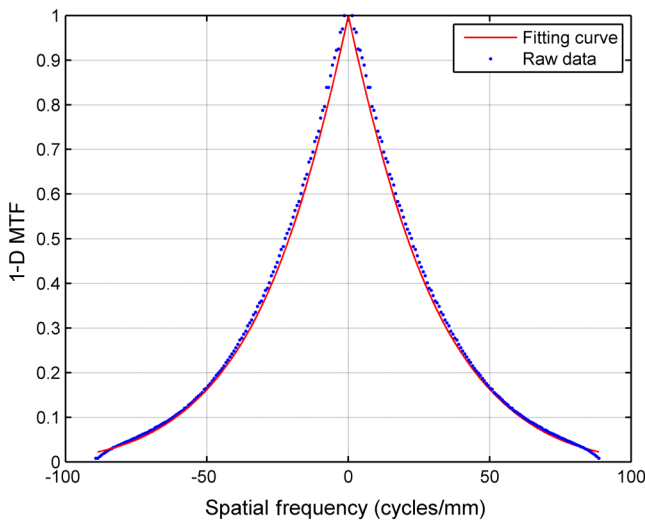


Fig. 10 Raw data of 1-D MTF and curve fitted with polynomials.

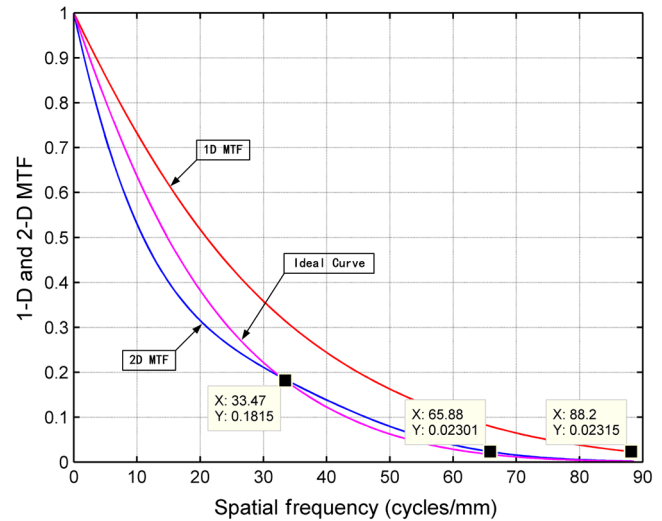


Fig. 12 The comparison of 1-D and 2-D MTF.

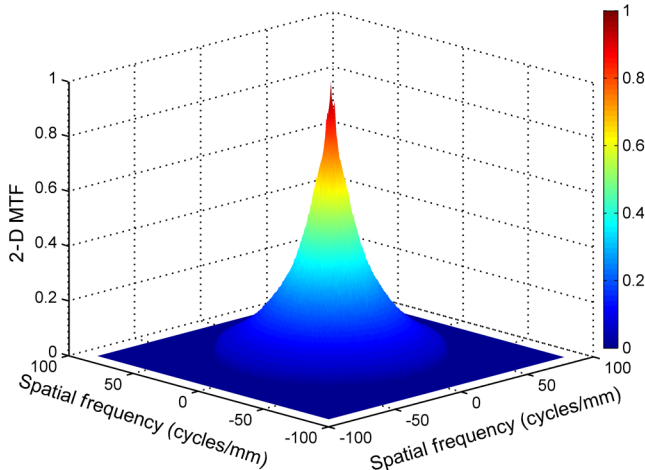


Fig. 11 2-D MTF.

curve at frequency  $f$  is equal to that of the 1-D MTF at frequency  $\sqrt{2}f$ . Also, when comparing with the 2-D MTF curve (in blue), these two curves do not strictly obey the relationship in Eq. (9) except at one point, which is located at about  $0.38f_c \approx 33.47$  cycles/mm. The 2-D MTF curve will be lower than the ideal curve when  $f < 0.38f_c$  and will be higher than it when  $f > 0.38f_c$ . These results are not completely consistent with the conclusions for an ideal system when considering various aberrations in the practical systems since these aberrations will be reflected in the 2-D MTF measurement results.<sup>20</sup>

#### 4 Conclusions

The relationship between 1-D and 2-D MTF has been discussed in theory and investigated in an experiment based on the random target method. The theoretical and experimental results show that the 2-D MTF's values and cutoff frequency are lower than their counterparts in 1-D MTF, and that 2-D MTF can provide more comprehensive information

than the 1-D MTF does since it covers the 2-D frequency domain.

The major contributions of this work are that, to the best of our knowledge, we take the average of the 2-D FFT results of a sufficient number of random images; this is used as a noise reduction method in the 2-D MTF measurement of optical imaging systems for the first time. Also, we discuss the characteristics of 2-D MTF and 1-D MTF in terms of MTF values and cutoff frequency through comparing 2-D MTF with 1-D MTF in the same direction.

### Acknowledgments

This research was supported by the grant from the National Natural Science Foundation of China (Nos. 61275003 and 51327005), the Research Fund for Shenzhen Key Laboratory of LED Packaging (ZDSY20120619141243215), and Guangdong Project (No. 2012B091100014).

### References

1. M. Born and E. Wolf, *Principles of Optics*, 7th ed., CUP Archive, Cambridge (1999).
2. X. Chen et al., "Sensor modulation transfer function measurement using band-limited laser speckle," *Opt. Express* **16**(24), 20047–20059 (2008).
3. Y. Zhang et al., "Dynamic modulation transfer function: a method to characterize the temporal performance of liquid-crystal displays," *Opt. Lett.* **33**(6), 533–535 (2008).
4. X. B. Li et al., "An analysis of the knife-edge method for on-orbit MTF estimation of optical sensors," *Int. J. Remote Sens.* **31**(17–18), 4995–5010 (2010).
5. J. T. Olson, R. L. Espinola, and E. L. Jacobs, "Comparison of tilted slit and tilted edge superresolution modulation transfer function techniques," *Opt. Eng.* **46**(1), 016403 (2007).
6. G. D. Boreman and S. Yang, "Modulation transfer function measurement using three- and four-bar targets," *Appl. Opt.* **34**(34), 8050–8052 (1995).
7. J. R. Rogers, "Three-bar resolution versus MTF: how different can they be anyway?," *Proc. SPIE* **7071**, 707109 (2008).
8. X. Zhang et al., "Measuring the modulation transfer function of image capture devices: what do the numbers really mean?," *Proc. SPIE* **8293**, 829307 (2012).
9. E. Marom, B. Milgrom, and N. Konforti, "Two-dimensional modulation transfer function: a new perspective," *Appl. Opt.* **49**(35), 6749–6755 (2010).
10. H. Haim, N. Konforti, and E. Marom, "Performance of imaging systems analyzed with two-dimensional target," *Appl. Opt.* **51**(25), 5966–5972 (2012).
11. H. Haim, N. Konforti, and E. Marom, "Optical imaging systems analyzed with a 2D template," *Appl. Opt.* **51**(14), 2739–2746 (2012).
12. A. Daniels et al., "Random transparency targets for modulation transfer function measurement in the visible and infrared regions," *Opt. Eng.* **34**(3), 860–868 (1995).
13. S. M. Backman et al., "Random target method for fast MTF inspection," *Opt. Express* **12**(12), 2610–2615 (2004).
14. A. H. Lettington and Q. H. Hong, "Measurement of the discrete modulation transfer-function," *J. Mod. Opt.* **40**(2), 203–212 (1993).
15. A. Fernandez-Oliveras, A. M. Pozo, and M. Rubino, "Comparison of spectacle-lens optical quality by modulation transfer function measurements based on random-dot patterns," *Opt. Eng.* **49**(8), 083603 (2010).
16. E. Levy et al., "Modulation transfer function of a lens measured with a random target method," *Appl. Opt.* **38**(4), 679–683 (1999).
17. F. A. Navas-Moya et al., "Measurement of the optical transfer function using a white-dot pattern presented on a liquid-crystal display," *J. Eur. Opt. Soc.* **8**, 13029 (2013).
18. B. T. Teipen and D. L. MacFarlane, "Liquid-crystal-display projector-based modulation transfer function measurements of charge-coupled-device video camera systems," *Appl. Opt.* **39**(4), 515–525 (2000).
19. N. N. Evtikhiev, V. V. Krasnov, and S. N. Starikov, "A method of generating amplitude masks with a constant power spectra and using them to measure the two-dimensional modulation-transfer functions of optical systems," *J. Opt. Technol.* **80**(5), 294–300 (2013).
20. J. Q. Kang, X. M. Cheng, and Q. Hao, "Wavefront aberration detection: a new perspective," *Appl. Mech. Mater.* **496**, 1164–1168 (2014).

**Jiqiang Kang** received his master's degree in precise instrumentation from Tsinghua University, Beijing, China, in 2014. He is currently a PhD candidate at Hong Kong University.

**Qun Hao** received her PhD degree in precise instrumentation from Tsinghua University, Beijing, China, in 1998. She is currently a professor at Beijing Institute of Technology. Her research interests are freeform surface measurement, target pointing, and tracking, on which she has published at least 100 papers.

**Xuemin Cheng** received her PhD degree in photoelectric engineering from Beijing Institute of Technology, Beijing, China, in 2004. She is currently an associate professor at Tsinghua University, an OMNERC member, and also a committee member of the Opto-electronic-mechanical Committee in the Chinese Optical Society. Her research interests are optimization algorithms, and intelligent design of optical systems, on which she has published at least 41 papers.